AIAA 81-0257R

Solutions for Three-Dimensional Over- or Underexpanded Exhaust Plumes

V. N. Vatsa,* M. J. Werle,† O. L. Anderson,‡ and G. B. Hankins Jr.§
United Technologies Research Center, East Hartford, Conn.

An efficient method for solving the problem of a slightly under- or overexpanded supersonic jet exhausting into a subsonic coflowing stream is presented. This paper extends an earlier work on two-dimensional and axisymmetric flows to general three-dimensional flows with specific application to high-aspect-ratio slot jet flows. The viscous problem is rendered parabolic through a unique use of an approximate inviscid flow intrinsic coordinate system to estimate only the streamline curvatures. This inviscid problem is formulated in terms of linearized perturbation potentials for ease of solution. The results of application of this approach to axisymmetric and high-aspect-ratio slot jet flows will be presented.

Nomenclature

a,b,c,d	= generalized coefficients of differential equation
h_1,h_2,h_3	= metric coefficients in the coordinate directions x, y_2, and y_3, respectively
H_0	= total enthalpy
I,J,K	= indices to designate station numbers in the x, y_2, and y_3 directions, respectively
L	= reference length
M	= Mach number
p	= pressure
P_{r_T}	= turbulent Prandtl number
r	= ratio of adjacent mesh grid step sizes
T	= temperature
u_2,u_3	= velocity components in the coordinate directions y_2 and y_3, respectively
u	= streamwise velocity
x	= streamwise distance
y	= coordinate in transverse plane
γ	= ratio of specific heats
Δ	= step size or difference operator
δ	= a characteristic length
μ_T	= turbulent viscosity coefficient
ρ	= density
ϕ	= potential function
ψ	= stream function
ω	= vorticity

Subscripts

C	= inviscid core extent
℄	= centerline value
j	= jet value at exit plane
0	= stagnation or exit value
$1,2,3$	= streamwise, normal, and transverse directions, respectively
∞	= freestream value

Introduction

THE problem addressed here is that of predicting the detail flow structure in the jet plume that occurs when an under- or overexpanded hot jet exhausts into a cold coflowing subsonic stream (see Fig. 1). The ability to predict the details of the viscous mixing and cooling that take place at the jet interface is critical to determining the thermodynamic and acoustic signature of the vehicle producing the jet. It is therefore important to develop a reliable and efficient scheme for addressing this class of problems. There is a lack of reliable turbulence models for this class of under/overexpanded jet mixing problems: thus, only a simple algebraic turbulence model was employed in this study to allow assessment of the capabilities of the current solution procedure.

The overall goal of the current work was to develop an efficient solution technique for addressing both the cases of the axisymmetric and slot types of slightly under- or overexpanded hot jet flows in subsonic mainstreams. The approach used was a direct extension of a parabolic marching technique recently developed by Anderson[1] for internal axisymmetric flows at high Reynolds numbers. In that approach, Anderson introduced the concept of using an approximate intrinsic coordinate system to formally produce a parabolic composite set of equations that are valid throughout the inviscid and viscous regions of the flow. An implicit finite-difference algorithm based on Keller's box scheme[2] was employed to obtain fast, accurate solutions and numerous comparisons with experimental data have been achieved.[1,3]

In a recent paper,[4] this concept was extended directly to the axisymmetric case of a coflowing jet. To do this, the work first concentrated on developing the approximate intrinsic coordinate system required by the viscous flow solver. To this end, the inviscid flow was first predicted using perturbation theory to effect a rather simple construction of the plume shape. The accuracy of this inviscid solution was assessed through detailed comparison with more complicated solution

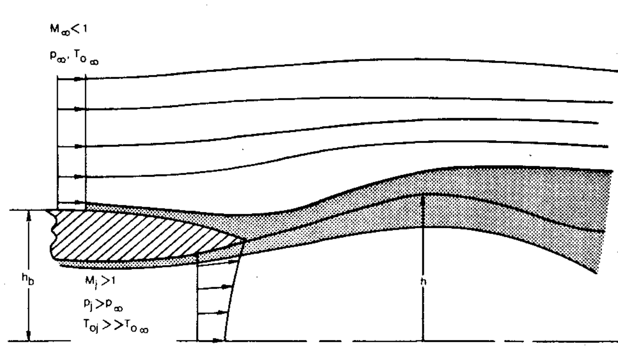

Fig. 1 Structure of plume flow.

Presented as Paper 81-0257 at the AIAA 19th Aerospace Sciences Meeting, St. Louis, Mo., Jan. 12-15, 1981; submitted March 3, 1981; revision received Jan. 4, 1982.

*Research Engineer. Member AIAA.

†Manager, Gas Dynamics and Thermophysics Laboratory. Member AIAA.

‡Senior Research Engineer. Member AIAA.

§Mathematical Scientist.

schemes that employ a method of characteristics representation of the jet flow. Thereafter, solution of the axisymmetric viscous plume problem was achieved for hot and cold subsonic jets exhausting into either still air or a subsonic stream. The turbulence model used was calibrated against experimental data for perfectly expanded subsonic jets. Thereafter, the applicability of the approach for under- and overexpanded jets was assessed through solution of hot supersonic jets for exit jet pressure ratios up to approximately 1.4 for flow into still air or a cold coflowing subsonic stream. Good comparisons were obtained with experimental data for axisymmetric underexpanded jet flows in a recent study[5] using this approach.

The axisymmetric solution technique described above has now been extended to the three-dimensional case for application to slot nozzle configurations. This work is based on the extension of Anderson's[1] axisymmetric internal flow technique to the case of axial three-dimensional flows by Anderson and Hankins[6] and Vatsa et al.[7] The resulting set of three-dimensional viscous flow equations has been solved using an implicit finite-difference technique for simultaneous solution of all of the flow properties. The basic numerical scheme has been assessed through application to: 1) incompressible turbulent axisymmetric jet configurations where analytical similarity solutions exist, 2) a 2×1 aspect ratio incompressible rectangular jet case where exact solutions for the farfield properties exist, and 3) axisymmetric compressible coflowing jet where independent solutions are available. The final test case studied was that of a slot jet of an aspect ratio of 53/1 with an exit Mach number of $M_j=1.55$ at an overpressure of $p_\infty/p_j=1.31$ and a temperature ratio of $T_{0j}/T_{0\infty}=3.02$. For this case, limited experimental data exist for assessing the current approach. In this study a detailed assessment is also made of the "equilibrium jet" approximation for the class of jet pressure ratios studied here. Comparisons are given between solutions of the full jet and equilibrium jet approaches as well as experimental data. From this it is found that this approximate approach provides a very accurate and efficient means of predicting under- or overexpanded jet plume characteristics.

Governing Equations

General Concept

The basic approach applied here for three-dimensional jet flows is essentially an extension of Anderson's work[1,3] on axisymmetric flows to three-dimensional flows as has been documented by Anderson and Hankins[6] and Vatsa et al.[7] The three-dimensional Navier-Stokes equations are formally parabolized in the streamwise direction based on the use of approximate intrinsic coordinates and a small secondary flow approximation similar to Blottner's[8] thin-channel approximation. This results in a set of equations that are elliptic in the transverse plane and parabolic in the streamwise direction. The present study represents the application of this approach to slightly under- or overexpanded jet flows exiting from rectangular slot nozzles and represents a summary of results presented by Vatsa et al.[7]

Viscous Equations

The governing equations are presented here for the most general case of three-dimensional viscous jet flow. Writing the equations of motion in general orthogonal coordinates and applying small secondary flow approximations the following reduced set of equations are recovered.
Continuity:

$$\frac{\partial}{\partial x}(h_2h_3\rho u)+\frac{\partial}{\partial y_2}\left[\frac{h_1h_3}{h_2}\rho\frac{\partial\phi}{\partial y_2}\right]+\frac{\partial}{\partial y_3}\left[\frac{h_1h_2}{h_3}\rho\frac{\partial\phi}{\partial y_3}\right]=0 \tag{1}$$

Momentum:

$$\begin{aligned}&\frac{\partial}{\partial x}(h_2h_3\rho u^2)+\frac{\partial}{\partial y_2}\left[\frac{h_1h_3}{h_2}\rho u\frac{\partial\phi}{\partial y_2}\right]\\&+\frac{\partial}{\partial y_3}\left[\frac{h_1h_2}{h_3}\rho u\frac{\partial\phi}{\partial y_3}\right]+\frac{\partial\psi}{\partial y_3}\frac{\partial u}{\partial y_2}-\frac{\partial\psi}{\partial y_2}\frac{\partial u}{\partial y_3}+h_2h_3\frac{\partial p}{\partial x}\\&-\frac{\partial}{\partial y_2}\left[\frac{h_1h_3}{h_2}\mu_T\frac{\partial u}{\partial y_2}\right]-\frac{\partial}{\partial y_3}\left[\frac{h_1h_3}{h_3}\mu_T\frac{\partial u}{\partial y_3}\right]=0\end{aligned} \tag{2}$$

Transverse pressure:

$$\begin{aligned}&\frac{-\partial}{\partial y_2}\left(\frac{h_1h_3}{h_2}\frac{\partial p}{\partial y_2}\right)-\frac{\partial}{\partial y_3}\left(\frac{h_1h_2}{h_3}\frac{\partial p}{\partial y_3}\right)\\&+\frac{\partial}{\partial y_2}\left(\rho u^2\frac{h_3}{h_2}\frac{\partial h_1}{\partial y_2}\right)+\frac{\partial}{\partial y_3}\left(\rho u^2\frac{h_2}{h_3}\frac{\partial h_1}{\partial y_3}\right)\\&+\frac{\partial}{\partial y_2}(h_1\rho\omega)\frac{\partial\phi}{\partial y_3}-\frac{\partial}{\partial y_3}(h_1\rho\omega)\frac{\partial\phi}{\partial y_2}\\&-\frac{\partial}{\partial y_2}\left(\frac{h_3}{h_2}\frac{\partial\psi}{\partial y_2}\omega\right)-\frac{\partial}{\partial y_3}\left(\frac{h_2}{h_3}\frac{\partial\psi}{\partial y_3}\omega\right)=0\end{aligned} \tag{3}$$

Energy:

$$\begin{aligned}&\frac{\partial}{\partial x}(h_2h_3\rho uH_0)+\frac{\partial}{\partial y_2}\left[\frac{h_1h_3}{h_2}\frac{\partial\phi}{\partial y_2}\rho H_0\right]\\&+\frac{\partial}{\partial y_3}\left[\frac{h_1h_2}{h_3}\frac{\partial\phi}{\partial y_3}\rho H_0\right]+\frac{\partial\psi}{\partial y_3}\frac{\partial H_0}{\partial y_2}-\frac{\partial\psi}{\partial y_2}\frac{\partial H_0}{\partial y_3}\\&-\frac{1}{P_{r_T}}\left\{\frac{\partial}{\partial y_2}\left[\frac{h_1h_3}{h_2}\mu_T\frac{\partial H_0}{\partial y_2}\right]+\frac{\partial}{\partial y_3}\left[\frac{h_1h_2}{h_3}\mu_T\frac{\partial H_0}{\partial y_3}\right]\right\}\\&-\frac{P_{r_T}-1}{P_{r_T}}\left\{\frac{\partial}{\partial y_2}\left[\frac{h_1h_3}{h_2}\mu_T\frac{\partial}{\partial y_2}\left(\frac{u^2}{2}\right)\right]\right.\\&\left.+\frac{\partial}{\partial y_3}\left[\frac{h_1h_2}{h_3}\mu_T\frac{\partial}{\partial y_3}\left(\frac{u^2}{2}\right)\right]\right\}=0\end{aligned} \tag{4}$$

Vorticity:

$$\omega+\frac{1}{h_2h_3}\left[\frac{\partial}{\partial y_2}\left(\frac{h_3}{h_1h_2}\frac{1}{\rho}\frac{\partial\psi}{\partial y_2}\right)+\frac{\partial}{\partial y_3}\left(\frac{h_2}{h_1h_3}\frac{1}{\rho}\frac{\partial\psi}{\partial y_3}\right)\right]=0 \tag{5}$$

Vorticity transport:

$$\begin{aligned}&\frac{\partial}{\partial x}(h_2h_3\rho u\omega)+\frac{\partial}{\partial y_2}\left[\frac{h_1h_3}{h_2}\rho\frac{\partial\phi}{\partial y_2}\omega\right]\\&+\frac{\partial}{\partial y_3}\left[\frac{h_1h_2}{h_3}\rho\frac{\partial\phi}{\partial y_3}\omega\right]+\frac{\partial\psi}{\partial y_3}\frac{\partial\omega}{\partial y_2}-\frac{\partial\psi}{\partial y_2}\frac{\partial\omega}{\partial y_3}\\&+2\rho u\left[\frac{\partial u}{\partial y_3}\frac{\partial h_1}{\partial y_2}-\frac{\partial u}{\partial y_2}\frac{\partial h_1}{\partial y_3}\right]-h_2h_3\omega\frac{\partial}{\partial y_1}(\rho u)\\&-h_1\frac{\partial}{\partial y_2}\left[\frac{h_3}{h_1h_2}\frac{\partial}{\partial y_2}(h_1\mu_T\omega)\right]\\&-h_1\frac{\partial}{\partial y_3}\left[\frac{h_2}{h_1h_3}\frac{\partial}{\partial y_3}(h_1\mu_T\omega)\right]=0\end{aligned} \tag{6}$$

Equation of state:

$$p=\frac{\gamma-1}{\gamma}\rho\left(H_0-\frac{u^2}{2}\right) \tag{7}$$

The two transverse momentum equations have been replaced by the vorticity transport equation for the secondary vorticity and a pressure equation obtained by differentiating the transverse momentum equations. In addition, the transverse velocity is decomposed into irrotational and rotational components such that

$$u_2 = \frac{1}{h_2}\frac{\partial \phi}{\partial y_2} + \frac{1}{h_1 h_3 \rho}\frac{\partial \psi}{\partial y_3} \tag{8a}$$

$$u_3 = \frac{1}{h_3}\frac{\partial \phi}{\partial y_3} - \frac{1}{h_1 h_2 \rho}\frac{\partial \psi}{\partial y_2} \tag{8b}$$

When Eqs. (8) are substituted into the continuity equation, the rotational component ψ does not contribute to the mass flow balance and the irrotational component ϕ does not contribute to the vorticity.

Boundary Conditions

Equations (1-6) contain six unknowns, u, p, H_0, ϕ, ψ, and ω, each equation being of the Laplacian form in the cross plane. Thus, six boundary conditions of the form

$$af + b\frac{\partial f}{\partial y_n} = 0 \tag{9}$$

must be applied where y_n is normal to the boundary.

The freestream conditions are given as

$$p = p_\infty \qquad u = u_\infty \qquad H_0 = H_{0\infty}$$

$$\omega = 0 \qquad \psi = 0 \qquad \phi = \ln\left(\frac{r}{r_\infty}\right) \tag{10}$$

while at the jet centerline

$$\frac{\partial p}{\partial y_3} = 0 \qquad \frac{\partial u}{\partial y_3} = 0 \qquad \frac{\partial H_0}{\partial y_3} = 0$$

$$\omega = 0 \qquad \psi = 0 \qquad \frac{\partial \phi}{\partial y_3} = 0 \tag{11}$$

where r is the polar radius of the jet. Details of the derivation of these conditions can be found in Ref. 6.

Turbulence Model

A simple isotropic extension of the turbulence model employed for the axisymmetric problem in Ref. 4 has been used in the present study—it is essentially an eddy viscosity model capable of predicting the jet flows all the way from the potential core region to the fully developed turbulent region. The main difference between the axisymmetric and three-dimensional turbulence model is in the definition of δ, the characteristic length scale used in the turbulent viscosity relation

$$\mu_T = C\rho\delta(u_{\max} - u_{\min}) \tag{12}$$

where C is a constant to be defined and δ is taken as

$$\delta = \sqrt{\delta_2^2 + \delta_3^2} \tag{13}$$

As a direct analog to their two-dimensional equivalent, δ_2 and δ_3 should be established based on the velocity defects in the y_2 and y_3 directions, respectively. For very high-aspect-ratio jet flows, $\delta = \delta_2$ was used due to a lack of resolution in the y_3 direction. Alternately, one could use an approach similar to that of Sforza et al.,[9] where the constant C in the eddy viscosity relation was selected to be a function of the jet half-widths in the y_2 and y_3 directions. Such an approach would be expected to yield a smooth transition in the eddy viscosity as the flow develops from a rectangular to an axially symmetric jet.

For the general jet case the mixing process is assumed to take place in three principal regions, each with their own versions of the correct term to be used in Eq. (13). The three regions are the initial mixing region I (potential core region), a fully turbulent region III, and an intermediate or transitional region II.

The initial mixing region (region I) has been documented by Schlicting,[10] where analytical solution of this problem has been given in similarity variables. Here δ is taken as the distance between the two points in the shear layer where $[(u - u_{\min})/(u_{\max} - u_{\min})]^2$ varied from 0.1 to 0.9. By matching the measured width of the mixing zone, a value of 0.014 was obtained for the constant C.

For the fully turbulent region (region III), Hinze[11] has taken δ as the jet half-width and assigned C a value of 0.0256 on the basis of experimental data.

For the intermediate or transitional region, an approach similar to that of Chen[12] is employed where it is assumed that the flow becomes fully turbulent at $x = 2x_C$ where x_C represents the end of potential core region. It was assumed that the potential core ends when the centerline velocity of the jet differs by more than 1% from the jet exit velocity. With this, the eddy viscosity model used here can be summarized as

$$\mu_T = \begin{cases} \mu_{T_{\mathrm{I}}} & (x \le x_C) \\ (2 - x/x_C)\mu_{T_{\mathrm{I}}} + (x/x_C - 1)\mu_{T_{\mathrm{III}}} & (x_C \le x \le 2x_C) \\ \mu_{T_{\mathrm{III}}} & (x \ge 2x_C) \end{cases} \tag{14}$$

Numerical Method

The equations of motion presented above were first linearized by expanding in a Taylor series in the marching direction x to write that

$$(fg)^{I+1} = f^I g^{I+1} + f^{I+1} g^I - f^I g^I \tag{15}$$

After expanding all of the nonlinear terms, the full equation can be reduced to the index form

$$a_{LN}^M \frac{\partial^2 f^M}{\partial y_{N^2}} + b_{LN}^M \frac{\partial f^M}{\partial y_N} + c_L^M f^M + d_L = 0 \tag{16}$$

where the summation convention has been employed and

$M = 1,6$ variable number

$L = 1,6$ equation number

$N = 1,3$ coordinate direction

Note that only first derivatives appear in the marching direction so that here

$$a_{L1}^M \equiv 0 \tag{17}$$

The finite-difference grid is defined as

$$\Delta x(I) = x(I+1) - x(I)$$

$$\Delta y_2(J) = y_2(J+1) - y_2(J)$$

$$\Delta y_3(K) = y_3(K+1) - y_3(K) \tag{18}$$

At the marching station I, all of the transverse plane derivatives at a grid point I, J, K are evaluated according to the scheme

$$\frac{df}{dy_2}=\frac{f(I,J+1,K)-[1-\iota^2]f(I,J,K)-\iota^2 f(I,J-1,K)}{\Delta y_{2_J}+\iota^2\Delta y_{2_{J-1}}} \tag{19a}$$

$$\frac{d^2f}{dy_2^2}=\frac{f(I,J+1,K)-[1+\iota]f(I,J,K)+\iota f(I,J-1,K)}{[\Delta y_{2_J}^2+\iota^2\Delta y_{2_{J-1}}^2]/2} \tag{19b}$$

where

$$\iota=\frac{\Delta y_{N_J}}{\Delta y_{N_{J-1}}} \tag{19c}$$

Similar expressions are used for obtaining derivatives in the y_3 direction. The resulting set of linear algebraic equations were solved using a block successive under-relaxation scheme.

Results and Discussion

In order to perform an assessment of the accuracy and reliability of the three-dimensional algorithm described above, the following test cases were investigated. Two classical incompressible cases were first studied to allow comparison with analytic results. Next, comparisons with previous axisymmetric underexpanded jet solutions were studied to assess compressibility effects and the equilibrium jet approximation. Finally, a high-aspect-ratio overexpanded slot jet was studied to assess the full three-dimensional capability of this approach.

Solutions for two classical incompressible problems (an axisymmetric free jet and a farfield rectangular jet) were obtained using the current approach and have been presented by Vatsa et al. in an earlier paper.[13] It was shown in Ref. 13 that these solutions compared very well with known analytic results. As a result of this work, it was concluded that the current approach can successfully capture an axisymmetric flow on a Cartesian grid and predict the development of a rectangular jet into an axisymmetric flow, thus validating the ability of the overall approach to represent these two critical aspects of any general jet exhaust flow configuration. The following problems further verify the ability of this method to represent mismatched exit pressure jet flows with significant compressibility effects.

Axisymmetric Underexpanded Jet

The following viscous problem was studied to verify the ability of the three-dimensional code to solve nonrectangular jet flows with mixed subsonic and supersonic streams. To this end an axisymmetric underexpanded supersonic jet configuration was solved in rectangular coordinates, and solutions compared with those obtained from the axisymmetric approach presented in Ref. 4. This provides a most severe test for the three-dimensional code since it involves significant three-dimensional gradients, the mixing of a hot supersonic and cold subsonic flow, and realistic lateral pressure gradients. The case chosen for comparison was that of a supersonic jet with $M_j=1.9$ exhausting at a pressure ratio of $p_j/p_\infty=1.1$ and temperature ratio of $T_{0j}/T_{0\infty}=11.8$ into a subsonic stream at $M_\infty=0.8$. The three-dimensional solutions were obtained in a rectangular grid using 441 points in the cross plane (21 each in the y_2 and y_3 directions) with a grid distribution set up as $\Delta y_{2,3}=0.1\ y_j$ for $y\leq y_j$ and a geometric progression with a stretching constant of 1.20 for $y_{2,3}>y_j$. The current axial grid length was taken as $\Delta x=0.115\ y_j$ for both the three-dimensional and the axisymmetric calculations. The resulting centerline pressure and temperature comparisons are shown in Fig. 2 for the first portion of the initial cell length of the plume. Virtually no differences were encountered in the centerline pressure levels and only a small

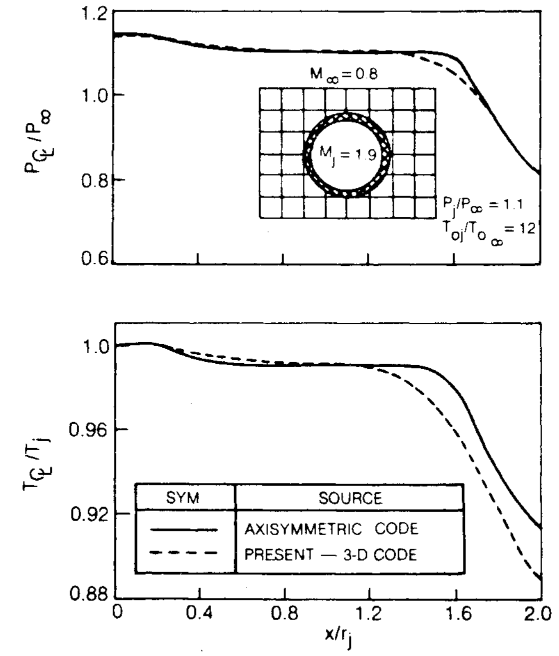

Fig. 2 Accuracy assessment for axisymmetric underexpanded jet.

difference was observed in the temperature field—this being manifest as a slight shift in the position at which the temperature felt the exit expansion wave.

Equilibrium Jet Model: Axisymmetric Assessment

Before proceeding to the final three-dimensional jet problem, an assessment is first made here of the equilibrium jet approximation for slightly over- or underexpanded coflowing jets. This general concept has been employed by previous authors (see Ref. 14 for example) and involves the use of an equivalent matched exit pressure case to estimate the mixing process of the mismatched pressure case. The analytical basis for this approach is to be found in the inviscid jet solutions presented in Ref. 4. There it was pointed out that the slightly mismatched jet case produces a plume cell structure that oscillates about a jet width equal to that obtained through expansion of the jet exit gas to the freestream pressure level. The utility of this concept for pressure and temperature predictions is assessed here through comparison with the axisymmetric predictions of Ref. 4 and data of Ref. 15. For these cases the lateral grid distribution used 91 points across the shear layer with $\Delta y_2/y_j=0.072$. The longitudinal step was taken as $\Delta x=0.058\ y_j$ for the underexpanded jet calculation. Results obtained with the equilibrium jet model are shown in Fig. 3 to virtually reproduce the measured and predicted underexpanded jet total pressure and temperature distributions at the downstream measuring station. These latter results were obtained with virtually the same transverse grid spacing but with an axial grid spacing of $\Delta x/y_j=0.29$, which is five times larger than that used for the underexpanded jet calculation. Clearly, these results indicate that this approximation gives a very good overall picture of the plume flow characteristics and that this approach should always be employed unless the details of the flow structure are needed.

Overexpanded Slot Jet

The final test case studied was that of a "two-dimensional" supersonic ($M_j=1.55$), hot ($T_{0j}=906$ K) jet exhausting to an ambient cold ($T_{0\infty}=311$ K) state at an overpressure ratio ($p_\infty/p_j=1.3$). For this case the slot exit width was 0.015 m and the slot span was 0.81 m, producing a virtually two-dimensional environment. Limited experimental results have been reported for this case by Thayer,[16] so that a qualitative assessment of the current approach can be made.

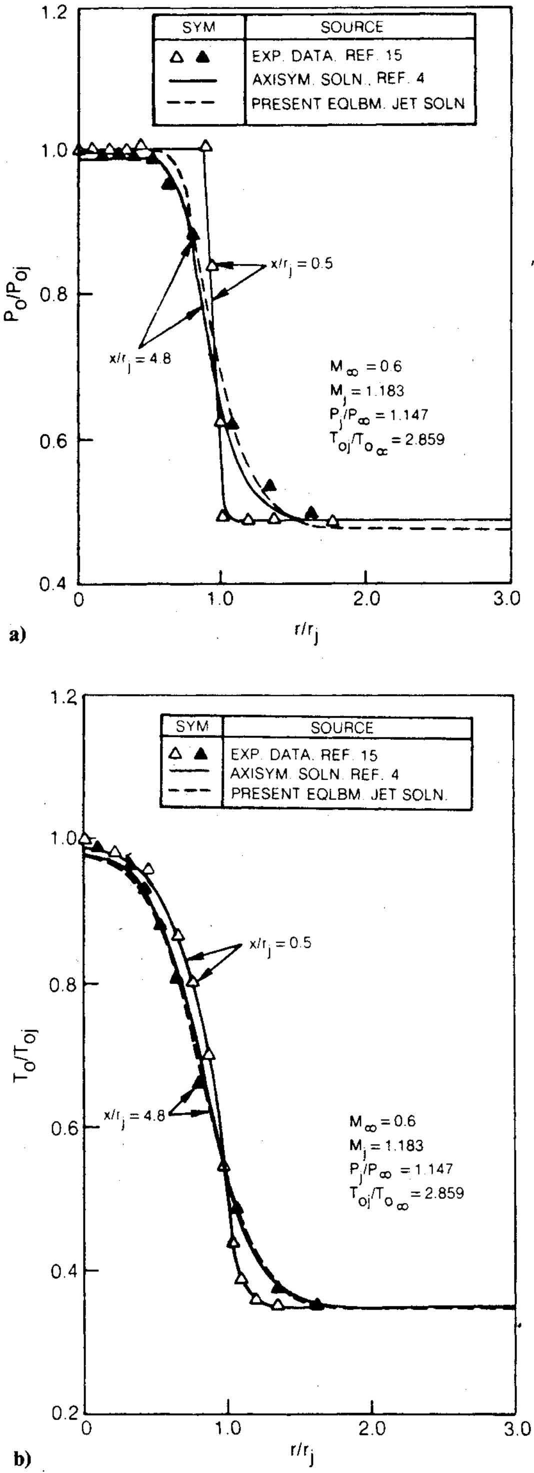

Fig. 3 Underexpanded coflowing jet: a) stagnation pressure distribution, b) stagnation temperature distribution.

The distribution of grid points for the finite-difference solution of the viscous equations is somewhat more complicated for this case. Concentrating first on the transverse plane, the vertical distribution was established for an essentially two-dimensional flowfield. In particular, the mesh was set so that $\Delta y_2/y_j = 0.15$ for $y_2 \leq 1.66\ y_j$ while for y_2 larger than this a geometric progression with a stretching constant of 1.26 was used to set Δy. Twenty-five grid points were used in this direction to capture the full flowfield.

For the spanwise direction, only 10 grid points were employed since gradients in this direction were expected to be relatively small and the details of the jet edge mixing suspected to be of secondary importance. Six of the grid points were located uniformly across the nozzle span with the remaining four located in the freestream region at the same grid spacing.

For this test case, the inlet flow conditions were estimated from the configuration description supplied in Ref. 16. These profiles are shown as the solid curves in Fig. 4 where a slight discrepancy is observed in the experimental centerline temperature values from the vertical and transverse measurements. These differences are apparently due to the fact that these measurements were taken at different times during the testing procedure[17] and thus they indicate a possible drift in jet stagnation temperature levels. Therefore, all subsequent comparisons with experimental data must be considered of a qualitative nature only.

Solutions have been obtained for this test case for four different levels of approximation. The first of these involves use of the full three-dimensional approach applied to the overexpanded jet conditions, the second involves use of the three-dimensional method for the equilibrium jet approach, the third uses a two-dimensional approximation applied to the overexpanded jet, and the fourth a two-dimensional approximation for the equilibrium jet. The initial conditions for each of these cases is shown in Fig. 4. Note that vertical distributions indicate that the two- and three-dimensional approaches employed the same distributions and that the equilibrium jet approximation accounts for the overpressure induced necking down by initializing with a narrower profile. In the spanwise plane, the two-dimensional solutions naturally show no variations with distance y_3. The three-dimensional equilibrium jet profile again shows a necking down due to the overpressure ratio.

The results of the calculations and comparisons with experimental data at a station 0.305 m aft of the nozzle exit are also shown in Fig. 4. Several things are immediately clear from an overall review of these figures: first, that the data comparisons are acceptable, showing only an expected qualitative agreement; and second, that all four of the model solutions produced essentially the same vertical distributions of total temperature. The only differences of any consequence are shown in the total pressure distributions where, as indicated in Fig. 4a, the equilibrium jet model shows a smoother and lower difference in initial profiles shown in the figures. It must also be recalled that the data are suspect due to measurement difficulties, while the analytical solutions have a limitation due to the usage of a simple algebraic turbulence model. Nonetheless, the favorable comparisons of Fig. 4 are encouraging and indicate that the overall approach employed here provides an effective means of predicting these three-dimensional jet mixing flows. It is anticipated that the use of a more sophisticated turbulence model such as the two-equation turbulence models used by Barton et al.[18] and McGuirk and Rodi[19] for predicting development of slot jet flows in conjunction with the present method could enhance the quantitative level of the three-dimensional jet flow predictions reported herein.

With regard to the four model comparisons of Fig. 4, it is quite clear first that equilibrium jet approximation is fully adequate for this class of flows since it produced an excellent representation of the overexpanded jet calculation. In addition, it is seen that the two-dimensional solutions presented in Fig. 4 virtually reproduce the three-dimensional results over the jet gas flow regions. This is critically important for it clearly indicates that for this class of slot jet flows, the computational effort can be reduced by an order of magnitude without significant loss of accuracy.

With regard to the computational effort required for these solutions, several points should be made. First, for the full three-dimensional calculations with the transverse grid discussed above, the calculation scheme required approximately 30 s of CPU time per axial station on a UNIVAC 1110 computer. All the cases shown here were run with a variable step size in the streamwise direction (Δx varied 0.0038

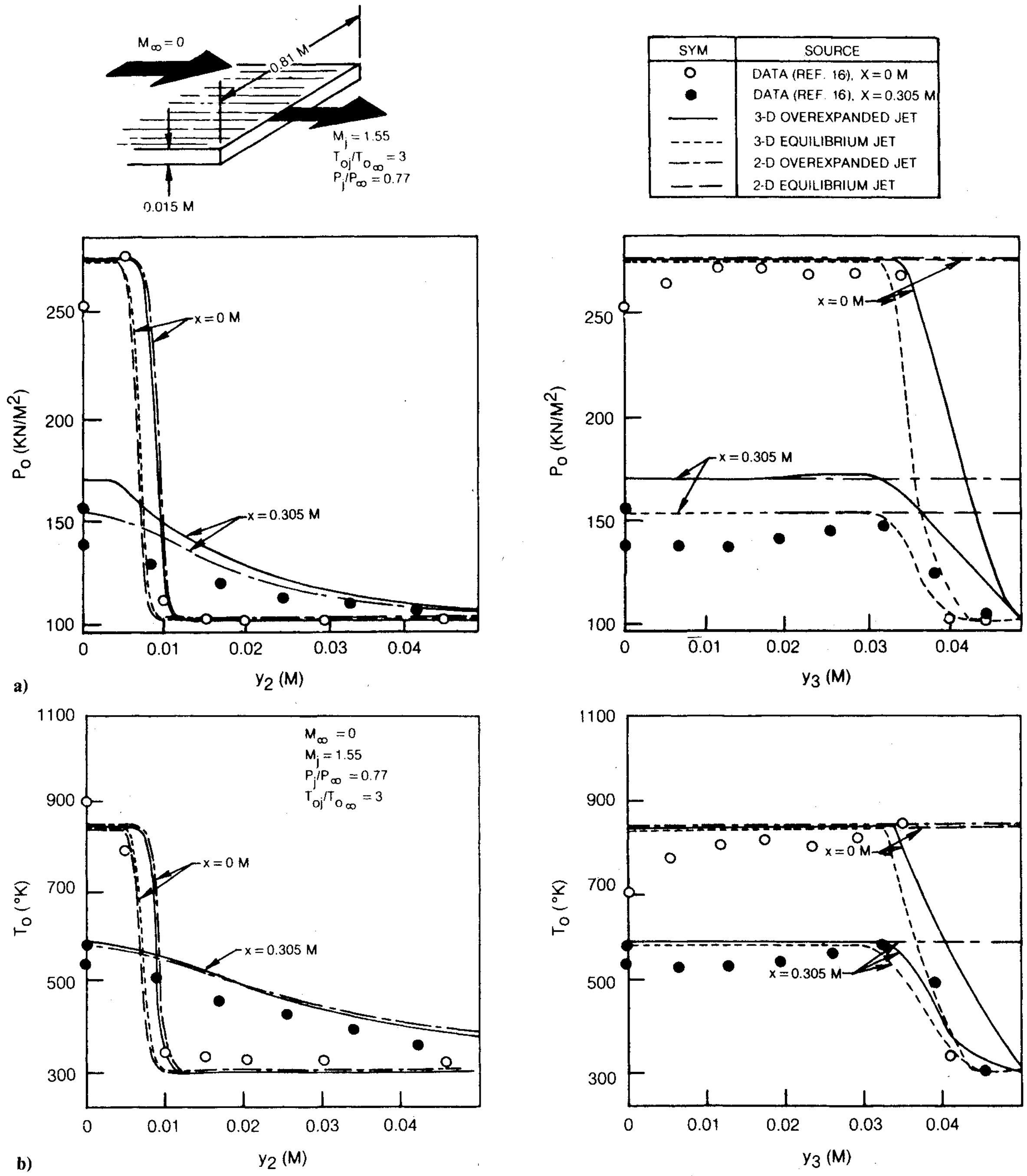

Fig. 4 Slot jet near field representation: a) pressure distribution, b) temperature distribution.

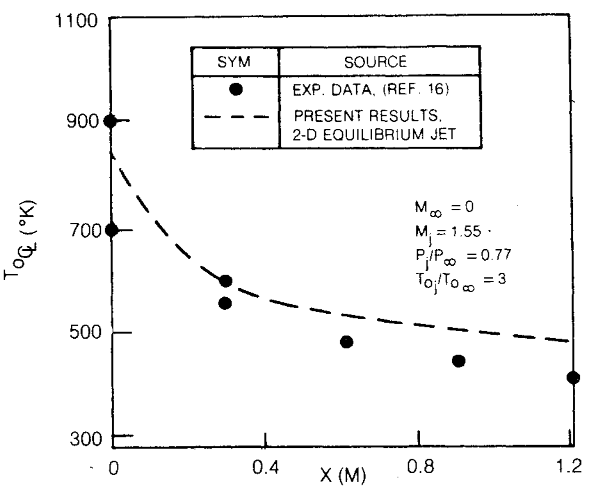

Fig. 5 Slot jet centerline temperature decay.

to 0.01524 m) and it required 28 streamwise stations to march to the 0.305 m station of Fig. 4 for a total computing effort of 14 min. The two-dimensional results shown in Fig. 4 were obtained from the present three-dimensional code by placing a reflective boundary condition at one of the off-centerline computational planes. Due to the current code structure, this required that five transverse planes be employed, thus providing only a factor of two reduction in the computer effort at the present time. The favorable comparisons of Fig. 4 clearly indicate the viability of this approach, which would warrant further code modifications that could easily reduce the computer effort by another factor of 5-10.

Since the two-dimensional equilibrium jet results of Fig. 4 were so encouraging, solutions have been continued further downstream using this approach. Figure 5 presents the centerline temperature comparisons at axial station 0.61 m ($x/h_j = 80$), 0.915 m ($x/h_j = 120$), and 1.22 m ($x/h_j = 160$) aft of the jet exit plane. Again, bearing in mind the experimental data limitations, these results are very encouraging and clearly indicate the viability of this simplified but very efficient approach for estimating the thermodynamic signature of large plume flow structures.

Conclusions and Recommendations

The detailed comparisons given here verify the current approach for calculating slightly under- and overexpanded coflowing slot jet plume characteristics. The parabolic marching method for representing viscous mixing was found to be accurate, stable, and efficient. The inviscid solution scheme employed to estimate approximate streamline curvatures was found to provide an accurate and simple representation of inviscid supersonic jets in coflowing subsonic streams. With regard to the viscous jet solution technique developed here, it was found that the equilibrium jet approximation provided an excellent representation of the jet plume characteristics for the class of problems considered here. Use of this approach greatly simplifies the analysis and provides a significant reduction in the computational effort required. It was also found that further efficiencies could be achieved by using a two-dimensional representation of the high-aspect-ratio slot jets considered here.

It is also apparent from this study that an experimental effort should be launched to acquire the data base necessary for a thorough assessment of the analytical methods currently at hand. Only a limited amount of data are available for the axisymmetric problem and virtually no detailed data are available for assessing the slot jet plume characteristics. A set of benchmark experimental studies should be conducted to provide a set of archival data for analytical model assessments. This experimental guidance is critically needed to provide a rational development of future analytical modeling for this type of high-aspect-ratio plume flows.

Acknowledgments

The authors wish to express their gratitude to several individuals who assisted in conducting this study: Dr. A. D. Gosman of Imperial College, London, England, for his assistance in turbulence modeling; Dr. B. Grosman of Grumman Aircraft Company for running his inviscid computer code to assist in the current approach; Herm Stevens and Bill Haynie of Pratt & Whitney, West Palm Beach, for their continued interest and guidance in the experimental data comparisons; and Dr. J. Carter for his interest and constructive guidance during the entire course of this study. This work was supported by the U.S. Air Force Flight Propulsion Laboratory under Contract F33615-76-C-2036 (subcontracted through Pratt & Whitney, West Palm Beach, Fla.), and the United Technologies Research Center's Corporate Research Program.

References

[1]Anderson, O. L., "Calculation of Internal Viscous Flows in Axisymmetric Ducts at Moderate to High Reynolds Numbers," *International Journal of Computers and Fluids,* Vol. 8, No. 4, Dec. 1980, pp. 391-412.

[2]Keller, H. B., "Accurate Difference Methods for Linear Ordinary Differential Systems Subject to Linear Constraints," *SIAM Journal of Numerical Analysis,* Vol. 6, No. 1, March 1969, pp. 8-30.

[3]Barber, T. J., Ragahuraman, P., and Anderson, O. L., "Evaluation of an Analysis for Axisymmetric Internal Flows in Turbomachinery Ducts," Paper presented at Symposium on Primary, Non-Rotating Passages in Turbomachines, ASME Winter Annual Meeting, Dec. 1979; in *Flow in Primary Nonrotating Passages in Turbomachines,* edited by H. J. Herring, A. Soter, and G. W. Steltz, pp. 107-114..

[4]Vatsa, V. N., Werle, M. J., and Anderson, O. L., "Solution of Slightly Underexpanded Two-Dimensional and Axisymmetric Coflowing Jets," AIAA Paper 80-0006, 1980.

[5]Vatsa, V. N., Werle, M. J., and Anderson, O. L., "Solution of Slightly Underexpanded Two-Dimensional and Axisymmetric Coflowing Jets," *AIAA Journal,* Vol. 19, March 1981, pp. 303-310.

[6]Anderson, O. L. and Hankins, G. B., "Development of a Parabolic Finite Difference Method for 3-D High Reynolds Number Viscous Internal Flows," Paper presented at Meeting of ASME, Washington, D. C., Nov. 15-20, 1981; in *Computers in Flow Predictions and Fluid Dynamics Experiment,* edited by K. N. Ghia, T. J. Mueller, and B. R. Patel, pp. 119-128.

[7]Vatsa, V. N., Werle, M. J., Anderson, O. L., and Hankins, G. B., Jr., "Analysis of Slightly Under- or Over Expanded Axisymmetric and Slot Type Coflowing Jets," United Technologies Research Center, East Hartford, Conn., Rept. R80-217741-30, Dec. 1980.

[8]Blottner, F. G., "Numerical Solutions of Slender Channel Laminar Flow," *Computer Methods in Applied Mechanics and Engineering,* Vol. II, 1977, pp. 319-339.

[9]Sforza, P. M., Steiger, M. H., and Trentacoste, N., "Studies of Three-Dimensional Viscous Jets," *AIAA Journal,* Vol. 4, May 1966, pp. 800-806.

[10]Schlichting, H., *Boundary-Layer Theory,* 6th Ed., McGraw-Hill Book Co., New York, 1968.

[11]Hinze, J. O., *Turbulence,* 2nd Ed., McGraw-Hill Book Co., New York, 1975.

[12]Chen, C. Y., "Calculations of Far-Field and Near-Field Jet Noise," Paper 75-93 presented at AIAA 13th Aerospace Sciences Meeting, Jan. 20-22, 1975.

[13]Vatsa, V. N., Werle, M. J., Anderson, O. L., and Hankins, G. B., Jr., "Solutions for 3-D Over- or Under-Expanded Exhaust Plumes," Paper 81-257 presented at AIAA 19th Aerospace Sciences Meeting at St. Louis, Mo., Jan. 12-15, 1981.

[14]Sukanek, P. C., "Matched Pressure Properties of Low Altitude Plumes," *AIAA Journal,* Vol. 15, Dec. 1977, pp. 1818-1821.

[15]Robinson, C. E., Roux, J. A., and Bertrand, W. T., "Infrared Measurements on an Exhaust Plume From an Axisymmetric Afterbody Model at Transonic Mach Numbers," AEDC-TR-78-55, March 1979.

[16]Thayer, E. B., "Installed Turbine Engine Survivability Criteria," Test Report for Exhaust Plume Transverse Tests, PWA FR-9179, U. S. Air Force Contract F33615-76-C-2036.

[17]Stevens, H., Pratt & Whitney Aircraft Co., private communication, 1979.

[18]Barton, J. M., Birch, S. F., Forester, C. K., Paynter, G. C., Peersy, K. M., and Roberts, D. W., "The Computation of Complex Jet and Nozzle Flows," Paper presented at JANNAF 12th Plume Technology Meeting, Colorado Springs, Colo., Nov. 18-20, 1980.

[19]McGuirk, J. J. and Rodi, W., "The Calculation of Three Dimensional Turbulent Free Jets," Proceedings of Symposium on Turbulent Shear Flows, Pennsylvania State University, University Park, Pa., April 1977.